

## Analysis of Structure Destroyed Metal after Diffusion Heat Treatment

A M Apasov<sup>1</sup>, E V Kozlov<sup>2</sup>, S N Fedoseev<sup>1</sup>

<sup>1</sup>Yurga Institute of Technology, National Research  
Tomsk Polytechnic University Affiliate,  
26 Leningradsкая str., Yurga, Kemerovo region, RUS

<sup>2</sup>Tomsk State University of Architecture and Building,  
2 Solyanaya Square, Tomsk, Tomsk region, RUS

E-mail: mchmyti@rambler.ru, sfedoseev@tpu.ru

**Abstract.** It was accomplished research of the structure steel which carbonitriding and subsequent heat treatment was exposed for its cause's destruction to discover. For measure quality field of metal were used methods optical, appearing electronic microscopy and X-ray diffraction. Therefore one of the principal problems were research phase composition, grain and dislocation structure of a metal the gear teeth. Mechanism of rising hear cracks in the gear teeth on different stages her making and their trajectories of evolution were determined.

### Introduction

Uninterrupted operation of the conveyor in the development of powerful of underground layers black coal is associated with a high degree of reliability guarantee [1] drive of reducer, providing continuous feed conveyor belt and prevents blockages. This in turn can only be achieved by using the manufacturing process quality toothed gears working in shear, shear and buckling.

In connection with this problem development defect-free manufacturing technology toothed gear is very important. One method of increasing wears resistance and surface strength of a thermo chemical treatment, particularly nitro carburizing.

The study of the structure of nitro cemented of metal layer of the tooth gear is dedicated to the work [2], in which the established that with increasing distance from the surface nitro carburized layer is changed that is graded structure formed in the material. Work [3] was the logical continuation of the cycle of research, the results of which were published in the article [2]. At the same time the main objective is to continue the study of the gradient structure-phase states that are formed in the constructional alloyed steel 20H2N4A martensite class during the high temperature carbonitridation and subsequent heat treatment methods of X-ray diffraction and optical microscopy. At the same time been installed depending a structurally-phase states steel 20H2N4A on the distance from the surface carbonitridation. It is shown that low nitro carburizing and temper have a significant impact on the parameters of the gradient structurally-phase states.

In the article [4] are shown data that allow establishing the mechanism of nucleation of microcracks and to determine the trajectory of their development. Nevertheless, until now fabrication



stages remain unknown toothed gear, in which cracks arise and further features of their formation. The solution of this important problem and is dedicated to this research.

### Methodology Research

It is known that one of the basic metal imperfections subjected to carburizing and, in particular, nitriding are internal residual stresses. Thus in the surface layer compressive stresses are created in the mid – stretching. They can reach significant values and, especially, in a complex and variable configuration of parts, assemblies and products. Arising large internal stresses are sources of nucleation, formation and development of micro cracks, which then (under certain conditions) are transformed into a trunk to form crack-free surfaces, eventually leading to destruction of the product as a whole.

Carbonitriding work piece surface (gear teeth) of steel 20H2N4A was carried out at a temperature of 920 °C. Thus the thickness layer was nitro cemented 1500 microns. Thermal treatment of the samples after carbonitridation consisted of high tempering at 620 °C (1 hour), 820 °C by hardened in oil and tempering at a low 180 °C for 1 hr (Table. 1).

**Table 1.** Procedure of sampling for investigation

Number of the sample	Sample status	The distance from the surface of tested samples
Original	Condition on delivery	The Centre sample
Sample 8	Cutting the gear teeth	1) Surface; 2) 1.6 mm from the surface of the tooth
Sample 12	Nitro cementation 920 °C	1) Surface; 2) 2.07 mm from the surface of the tooth
Sample 13	Tempering at 620 °C, 1 hour	1) Surface; 2) 2.17 mm from the surface of the tooth
Sample 14	Hardening from 820 °C the oil	1) Surface; 2) 2.0 mm from the surface of the tooth
Sample 15	Tempering at 180 °C, 1 hour	1) Surface; 2) 2.1 mm from the surface of the tooth

For carrying out optical microscopy on the electric spark machine tooth portions were cut from the gear intact. They are represented in Figure 1, and thin sections are made in parallel (section 1, Figure 1a) and perpendicular (section 2, Figure 1b) nitro carburized plane relative to surface of the tooth. Grinding conducted to remove traces of spark erosion. To create a mirrored surface sample is subjected to electrolytic polishing. Wherein:

1. For detection of microcracks applied electrolytic etching in a supersaturated solution of chromic anhydride in H<sub>3</sub>PO<sub>4</sub>.
2. The grain structure is determined by electrolytic etching in a 10% HCl solution.
3. The structure set Carbide resulting samples electrolytic etching in 50% solution of hydrochloric acid.

Subsequently, the prepared samples were investigated by metallographic microscope MIM-10 at magnifications of 50, 100, and 380 times. The increase to 1500-fold was necessary for the manufacture of microstructures pictures.

Based on optical microscopy and solutions structure nitro cemented zones were identified layer, the shape and dimensions of the real and hereditary grain size and location coarse carbonitrides, the presence of microcracks and their trajectory.

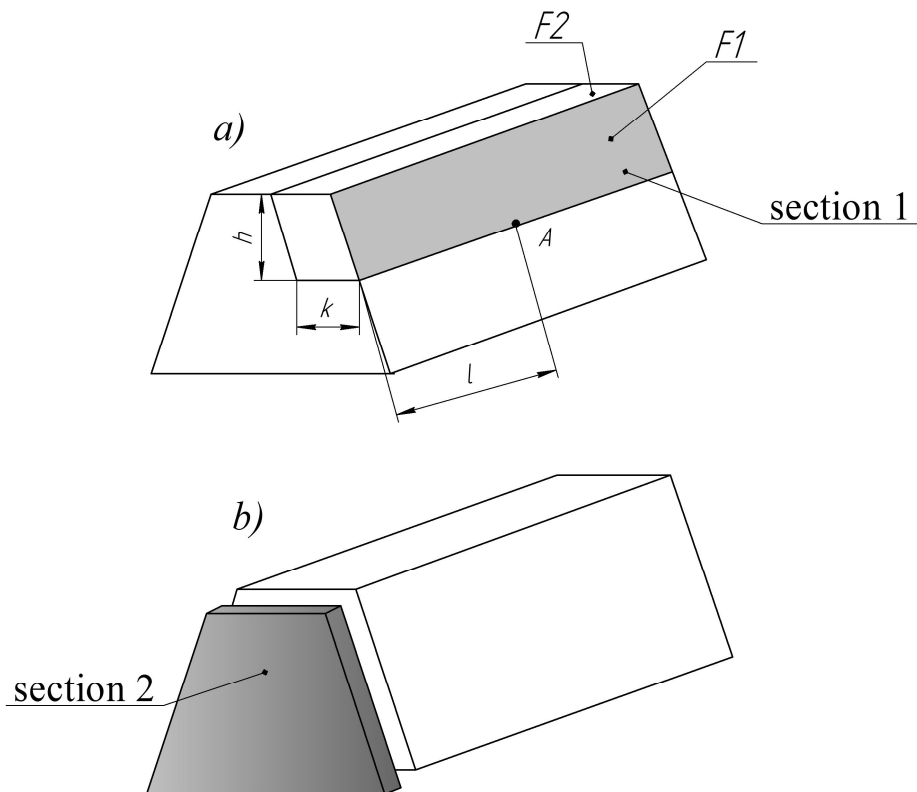


**Figure 1.** Scheme of cutting samples from the gear tooth for metallography, electron microscopy and X-ray analysis (section 1) and intaglio (section 2) in the electric spark machine.

A – area of research material (by electron microscopy and X-ray analysis) arranged on different surfaces of the tooth:  $h = 4,5$  mm;  $l = 15$  mm;  $k = 0$  (tooth surface – F1) and 2 mm (F2)

X-ray diffraction (XRD) sample made by X-ray diffractometer DRON-1.5 automatic scanning X-ray beam angles in the range from 19 to 150 degrees in the filtered  $Fe-K\alpha$ -radiation. Recording was carried out in automatic mode on a chart tape rate 1/2 degree per minute. The X-ray indicates the reflexes to determine the main phase components. Using the main diffraction maxima of  $\alpha$ -Fe and  $\gamma$ -Fe phase using known techniques allowed the calculation of lattice parameters (extrapolation  $\cos 2\alpha$  function), internal microdistortions and microtension type II, as well as hold on to texture analysis (reference data taken from [5, 6]).

From the analysis of the broadening of diffraction maxima of were obtained information about microdistortions and sizes of coherent scattering of the crystal lattice of the main phase units. The broadening of diffraction maxima of due to three factors: the finite width of the spectral line ( $Fe-K\alpha$ ), geometric shooting conditions and the state of the test sample [7]. The contribution to the broadening of reflex due to the imperfection of the crystal, called the true physical broadening of the X-ray line  $\beta$  ( $2\theta$ ). It is obtained by comparing the width of the reflex of the crystal with the width of the reflex from the reference defect-free sample. As a reference was used single crystal of chemically pure of the annealed iron.

Performed by X-ray phase analysis was qualitative and quantitative. Filing [5, 6] were used in conducting the qualitative phase analysis. As indicate the x-ray reflexes to determine the main phase components. Quantitative phase analysis was characterized on the basis of the integrated intensity of the diffraction lines of values. Having defined the texture relative intensity of the reflection (110)  $\alpha$ -Fe to the intensities of the reflexes (200), (211) and (220) of the same phase, followed by comparison with reference intensity ratio of  $\alpha$ -Fe. The intensity of the reflection (110)  $\alpha$ -Fe is taken as 100%.

Transmission electron microscopy (TEM) was performed on thin foils. The thin metal plates were cut from the different layers of the tooth (Figure 1a) parallel to the surface of the nitro cemented layer. Cut off to the electric spark machine metal plate thickness of 0.25 mm ~ previously been chemically cleaned by cutting traces in H<sub>2</sub>O<sub>2</sub> solution with the addition of a few drops of HF. Then realized their thinning electrolytic ally in a supersaturated solution of chromic anhydride in N<sub>3</sub>PO<sub>4</sub> to a thickness of ~ 0.17 m and viewing electronic microscope type EM-125 and EM-125K at an accelerating voltage of 125 kV. In this operation an increase in the electron microscope column ranged from 8.000 to 25.000 times. A final increase was achieved by using photographic printing.

To identify the phases present in the metal diffraction analysis was applied using the darkfield technique. The phase analysis carried out in accordance with the equilibrium diagrams of Fe-C-N, Cr-C-N and Ni-C-N and other iron alloys ternary diagram [8, 9]. When the diffraction pattern analysis verified the possible existence in the nitro carburized layer of the order of 30-35 table phase.

Images of thin metal structure used for:

- Classification of its morphological features;
- Determining the size, volume fraction and places of localization of secondary phases and discharge;
- The definition of scalar  $\rho$  and  $\rho_{\pm}$  excess dislocation density;
- Establishing the value of the amplitude of the curvature-torsion  $\alpha$  and torque stress  $\tau$ .

It has been viewed by a significant area of the foil and captured 30 to 40 micrographs and micro diffraction paintings to them for each test sample of a particular layer. The scalar dislocation density  $\rho$  measured by the cross-section [10]. Excessive density of dislocations in the local areas of the sample is determined by the curvature-torsion of the crystal lattice [11-13]:

$$\rho_{\pm} = \frac{1}{b} = \frac{d\varphi}{d\ell}, \quad (1)$$

where  $b$  – the Burgers vector,  $d\varphi/d\ell$  – the gradient of disorientation, i.e. orientation change with the movement of a particular plane on the model,  $\varphi$  – angle,  $\ell$  – distance. Direct measurements found that the width of the Bragg reflection for the elements of the first period is about 10 [14].

Therefore, by measuring the width of extinction contour curvature-torsion  $\Delta\ell$ , you can define  $d\varphi/d\ell$  from the condition:

$$\frac{d\varphi}{d\ell} = \frac{\Delta\varphi}{\Delta\ell} = \frac{1^{\circ}}{\ell}. \quad (2)$$

## Results and Discussion

Final thermal processing gear (hardening and subsequent low tempering) crushed ferrite grains in the study began. The size and orientation of the grains are extremely important for the problem of formation of microcracks, as well as for stress control material strength.

Shredding grain size increases the metal fracture [15], but it does not solve the whole problem.

The study 20H2N4A steel structural in all states except the original contains cracks. Their number varies according to the heat treatment and the distance from the surface of the gear tooth. These cracks are divided into three types:

1. the cleavage fracture;
2. quasi-cleaved fracture,
3. crack ductile fracture.

It was found that the most common fractures quasi-cleaved and ductile fracture.

Structure of cracks in the test steel 20H2N4A [4] is fundamentally different from the classical structure of the metal circuit with crack [4], which generates ahead of itself a small plastic zone with a

certain dislocation density. This area is surrounded by the elastic stress unreformed metal. Away from stress cracks in the metal are absent.

According to scheme [4], all the metal previously is deformed and has high dislocation density. At the mouth of the crack forming a special zone with a high level of elastic stress fields and increased the scalar dislocation density. In this zone, the elastic deformation much greater than metal plastic. In the rest of the metal, both the deformation contribution commensurate. In particular, the study steel 20H2N4A crack length ranges from 1.0 to 4.0 microns, and the length of the zone ahead of it – 0.5–7.0 mm. The density of dislocations in elastic stress zone may exceed the average density of dislocations in 1.5–2 times.

It is established that after the first nucleation microcracks occurring when cutting the teeth, their parameters increase after each subsequent heat treatment. It can be noted that the metal embrittlement, begun after cutting of gear teeth on the gear cutting, developed after each subsequent heat treatment.

Measurement of internal stress fields was carried out by X-ray analysis and transmission electron microscopy. It has been shown that the resulting gradual voltages of heat treatment processes increase, without exceeding 1000 MPa. This value critical and indicates the start of the fracture process because tensile strength of the test steel is approximately 1000 MPa. Since there is heterogeneity of internal stress fields throughout the volume of metal gears, it is the peak (maximum) voltages will serve as real sources of nucleation of microcracks.

In the zone located ahead of the front propagating the crack, the maximum stress level equal to 6500 MPa, reached after the nitrocarburizing process. Later in subsequent thermal treatments, this value decreases, remaining nevertheless significant ~ 4000 MPa.

This implies that only a high-strength metal in the way of propagating cracks will prevent the gear from damage.

Figure 2 shows more detailed information about the structure of the highly loaded areas [4] in the crack head. This figure shows the values of the amplitudes of the crystal lattice curvature-torsion  $\chi$  in two cases: 1 – directly at the crack tip; 2 – highly stressed at the boundary of zones 1 and zone 2 [4]. In zone 1 curvature-torsion elastic component of the crystal lattice ( $\chi$  resilient) is always greater than the plastic components ( $\chi$  ductile) that is provided by dislocations. In the zone 2, both components are comparable. The internal stress field in any of the areas is proportional to the total value of  $\chi$ , which is also given in this figure. The amount of stress in zone 1 for most types of heat treatment, either increasing or decreasing slightly. The maximum stress field are either after nitrocarburizing (sample 12), or after high-temperature tempering (sample 13), or after hardening (sample 14). Their numerical values are sufficient for the emergence of new cracks, as well as for the further development of already formed. The degree of hardening zones 1 and 2 is that the plastic of high stress relaxation difficult. Therefore, the main mechanism of stress relaxation data are the nucleation the processes of formation and development of cracks.

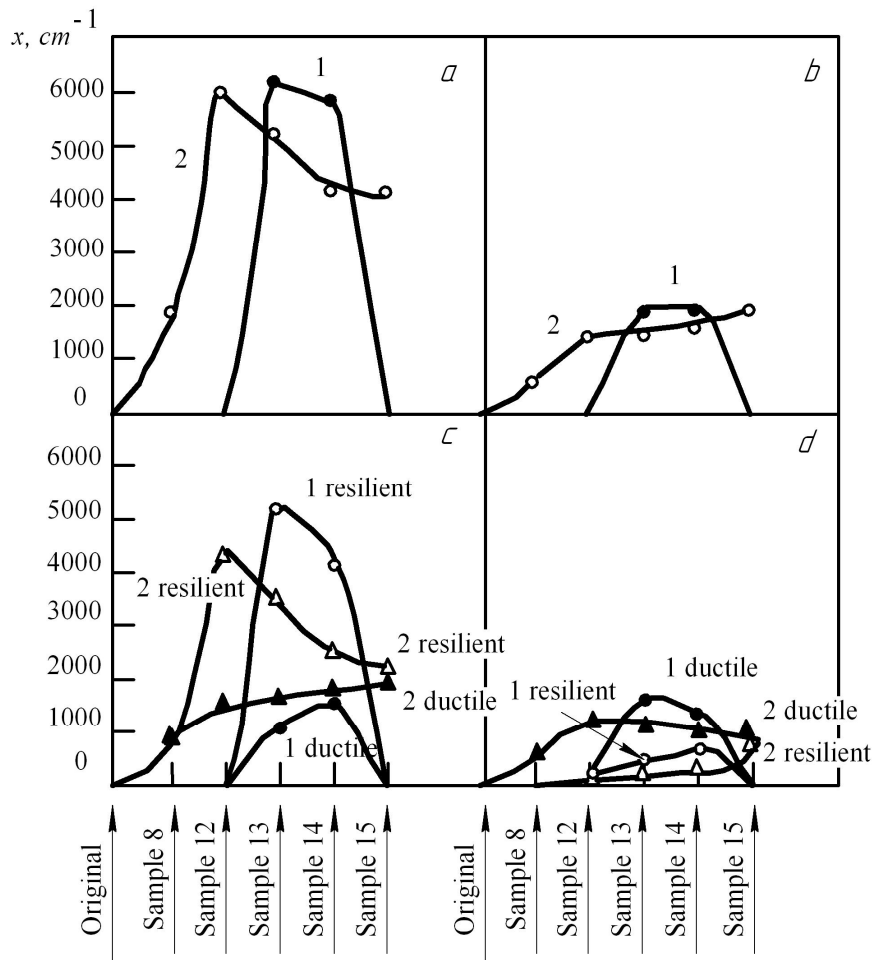


**Figure 2.** The change of curvature of the crystal lattice amplitude torsion  $\chi$ , measured by electron microscopy, depending on the heat treatment on the tooth surface of gears (1) and at a distance of ~ 2 mm from the surface of the tooth (2):  
 a, b - the crack in the head; b, d - in elastically deformed zone ahead of the crack;  
 a, b - the average value of the curvature-torsion  $\chi$  amplitude;  
 c, d - resilient (1 resilient, 2 resilient) and ductile (1 ductile, 2 ductile) components of the curvature-torsion amplitude

### Conclusion

As a result of studying the structure of the tooth nitro cemented layer of metal gears:

1. The quantitative characteristics of internal stress fields and microcracks.
2. The structure of the area ahead of the front of developing cracks.
3. It is shown that microcracks are generated already with cutting teeth and reach the most active state after nitrocarburizing, quenching and tempering high.
4. It was found that in all cases on the metal surface relaxation processes developed stronger. Therefore, activity of cracks inside the tooth above the metal, and the length of microcracks and their "sharpness" increases as the distance from nitrocarburizing layer into the metal.
5. It was determined that in all investigated conditions the metal has a significant amount of microcracks and the amplitude of such internal stress fields, which predicts a high probability of failure in the operation of the gears in the drive gear of the coal conveyor.

## References

- [1] Apasov A M, Galevsky G V 2008 Methods of research, testing, analysis and control in metallurgy and materialovedinii Tomsk 488
- [2] Kozlov E V, Popov N A, Malinovskaya V A, Apasov A M 2005 *J. Izvestia Ferrous Metallurgy* **8** 26-29.
- [3] Kozlov E V, Malinovskaya V A, Popova N A, Horseshoe V P Apasov A M 2006 *J. Izvestia Ferrous Metallurgy* **2** 33-36.
- [4] Abbasov A M, Apasov A A, Kozlov E V 2013 *J. Bulletin of the Tomsk Polytechnic universiteta* **2** 25-32/
- [5] Hu W, Yunxia W, Chenshuo M, Zhaolin Z 2014 *J. Applied Mechanics and Materials* **456** 406–410
- [6] Babcsan N, Leitlmeier D, Degischer H.P, Banhart J 2004 *J. Advanced Engineering Materials* **6** 421–428
- [7] Mao D, Edwards J R, Harvey A 2006 *J. Chemical Engineering and Science* **61** 1836–1845
- [8] Banhart J, Bellmann D, Clemens H 2001 *J. Acta Materialia* **49** 3409–3420.
- [9] Rodzevich A P, Kuzmina L V, Gazenaur E G, Krashenin V I 2014 *J. AIP Conference Proceedings* **1623** 519-522
- [10] Yang C C, Nakae H 2003 *J. Materials Processing Technology* **141** 202–206.
- [11] Ibragimov E A, Saprikin A A, Babakova E V 2014 *J. Advanced Materials Research* **1040** 764–767
- [12] Nokhrina O I, Rozhihina I D, Hodosov I E 2015 *J. IOP Conference Series: Materials Science and Engineering* **91** 12-17
- [13] Ferro P, Lazzarin P, Berto F 2012 *J. Materials Science and Engineering* **554** 122–128
- [14] Fedoseev S N, Mukhtar Z M 2015 *J. IOP Conference Series: Materials Science and Engineering* **91** 1–7
- [15] Nakae H, Fukami M, Kitazawa T, Zou Y 2011 *J. China Foundry* **8** 96–100